Renewable Energy 99 (2016) 107–117

Contents lists available at ScienceDirect

Renewable Energy

journal homepage: www.elsevier.com/locate/renene

Distributed generation integrated with thermal unit commitment considering demand response for energy storage optimization of smart grid

Harun Or Rashid Howlader*, Hidehito Matayoshi, Tomonobu Senjyu

Faculty of Engineering, University of the Ryukyus, 1 Senbaru, Nishihara-cho, Nakagami, Okinawa 903-0213, Japan

ARTICLE INFO

Article history:
Received 23 January 2016
Received in revised form
21 June 2016
Accepted 22 June 2016

Keywords:
Smart grid
Unit commitment
Renewable energy
Transmission constraint
Demand response
Battery energy storage system

ABSTRACT

This paper deals with an optimal battery energy storage capacity for the smart grid operation. Distributed renewable generator and conventional thermal generator are considered as the power generation sources for the smart grid. Usually, a battery energy storage system (BESS) is used to satisfy the transmission constraints but installation cost of battery energy storage is very high. Sometimes, it is not possible to install a large capacity of the BESS. On the other hand, the competition of the electricity market has been increased due to the deregulation and liberalization of the power market. Therefore, the power companies are required to reduce the generation cost in order to maximize the profit. In this paper, a thermal units commitment program considers the demand response system to satisfy the transmission constraints. The BESS capacity can be reduced by the demand response system. The electric vehicle (EV) and heat pump (HP) in the smart house are considered as the controllable loads of the demand side. The effectiveness of the proposed method is validated by extensive simulation results which ensure the reduction of BESS capacity and power generation cost, and satisfy the transmission constraints.

1. Introduction

Distributed renewable generators (DRGs) have gained interest in the power sectors in order to reduce the greenhouse gas emissions and power generation costs [1]. Due to the high penetration of the DRGs (e.g. wind generation, photovoltaic, biomass, hydro, and so on) and the deregulation and liberalization of the power markets, conventional power systems require significant amendments in planning and operation [2]. If a high penetration of DRGs is in the power grid, the power flow in the transmission line can be overloaded. As a result, it is difficult to maintain the balance between supply and demand sides and power system stability [3–7]. Further, the competition in power trading in the power sector increased owing to a lot of independent power producers. Therefore, electricity producers should use conventional thermal units efficiently so that they can lessen the operational cost and increase the profit. The aim of the smart grid is to integrate renewable sources into the conventional power system so that emissions and power generation costs can be reduced. Optimum operations of the high penetrating DRGs and thermal units, supply and demand controls, transmission constraints, and energy storage management are challenging for the smart grid system [8–14].

The revolution of industrialization and urbanization in the modern world has caused an increase in electricity demand. If a county has a high electricity demand, the power flow in the transmission line may become overloaded.Therefore, the thermal units commitment program has to consider the transmission constraints. The energy storage system (ESS) described in Refs. [15–17] that satisfies the transmission constraints for thermal units commitment program. The ESS can maintain power flow in the transmission line within a specific range and the efficient utilization of the ESS reduces the operation cost of thermal units. However, the installation cost of the ESSs is very high and some ESSs require a maintenance cost too [18,19]. Therefore, it can increase the power generation cost. Moreover, the capacity of the ESS should be optimized in order to reduce the installation as well as the power generation costs. Refs. [20–22] propose a spinning reserve to fulfill the transmission constraints for the thermal unit

* Corresponding author.
E-mail addresses: k148550@eve.u-ryukyu.ac.jp, h.h.howlader@ieee.org (H.O.R. Howlader).

http://dx.doi.org/10.1016/j.renene.2016.06.050
0960-1481/

Nomenclature

DRGs	Distributed renewable generators
PV	Photovoltaic
WG	Wind generation
BESS	Battery energy storage system
ESS	Energy storage system
HP	Heat pump
EV	Electric vehicle
V2G	Vehicle to grid
TS	Tabu search
LS	Local Search
SC	Solar collector
$maxR$	maximum benefits
TG_b	Thermal units benefits
TG_{cw}	Cost of thermal generator without demand response
TG_{cd}	Cost of thermal generator with demand response
$BESSc$	Battery energy storage system costs
S_{Bi}	Battery capacity
P_{Ii}	Inverter capacity
CI	Inverter capacity cost
TGc	Thermal units operating costs
SUC	Startup cost
P_{gi}	Thermal generators power
NG	Total thermal unit number
NB	Number of batteries
NI	Number of inverters
CB	Battery capacity cost
FC	Fuel cost
NT	Total scheduling period [hour]
i	Number of units
a_i	Fuel constant
b_i	Fuel constant
c_i	Fuel constant
t	Number of hours
T	Total hours
P_{Li}	Load demand
P_{PVdi}	Photovoltaic power from demand side
P_{WGi}	Power of wind generation
P_{PVi}	Photovoltaic power from supply side
P_{Bi}	Power of batteries
P_{EVi}	Power of electric vehicle
P_{HPi}	Power of heat pump
P_{gi}^{max}	Maximum power of thermal generator unit
P_{gi}^{min}	Minimum power of thermal generator unit
T_i^{on}	Minimum up time of unit
T_i^{off}	Minimum down time of unit
X_i^{on}	Continuously ON time of unit
X_i^{off}	Continuously OFF time of unit
P_{Bi}^{max}	Maximum power of battery
P_{Bi}^{min}	Minimum power of battery
S_{Bi}^{max}	Maximum state of charge
S_{Bi}^{min}	Minimum state of charge
$minF$	Minimum transmission constraints violation
P_{fij}	Power flow between nodes i and j
P_{fij}^{max}	Transmission constraints
P_{EVi}^{max}	EV battery maximum power
P_{EVi}^{min}	EV battery minimum power
S_{EVi}^{max}	Maximum state of charge of EV battery
S_{EVi}^{min}	Minimum state of charge of EV battery
P_{HPi}^{max}	HP maximum power
$T_{i(t=19)}$	Water temperature of storage tank at 19 O'clock

commitment program. The spinning reserve requires additional installation and maintenance costs for the power producer. Refs. [23–27] propose a power system using thermal units commitment and electric vehicle (EV) technology. The EV can deliver power to the power system through the vehicle to grid (V2G) technology. By introducing the EV into the thermal unit commitment program, the total operational cost of the power system has been reduced. A thermal units commitment program integrated with the demand response is proposed in Refs. [28–33]. The demand response can reduce thermal units cost and the transmission constraints are satisfied. Nowadays, uncertain power sources like DRGs are integrated with the conventional thermal generator, therefore, the power system has to maintain the transmission constraint as well as the balance between supply-demand sides. An ESS can fulfill these requirements. On the other hand, the advent of smart houses in the demand side, the capacity of the ESS and utilization of inconvenient thermal units can be reduced by the controllable loads such as EV and heat pump (HP) in smart houses. Furthermore, over the past few years, Tabu search (TS) has been applied to many difficult combinatorial optimization problems because TS is one of the most efficient heuristic techniques in the sense that it finds quality solutions in relatively short running time [34]. Usually, TS is an extension of classical local search (LS) methods, it can quite easily handle complicated constraints that are typically found in real-life applications. In fact, basic TS can be seen as simply the combination of LS with short-term memories. There are three basic elements of the TS that are search space, neighborhood solutions, and short-term Tabu lists. The search space of an LS or TS heuristic is simply the space of all possible solutions that can be considered (visited) during the search. A neighborhood solution is constructed to identify adjacent solutions that can be reached from current solution. Previously mentioned that TS is to pursue LS whenever it encounters a local optimum by allowing non-improving moves; cycling back to previously visited solutions is stopped by the use of memories, called Tabu lists, that record the recent history of the search, that is a key idea that can be linked to artificial intelligence concepts [35].

This paper proposes a smart grid system which consists of DRGs (e.g. wind generation (WG) and photovoltaic (PV)), thermal units and battery energy storage systems (BESSs) in the supply-side and a large number of residential and smart houses in the demand-side. A smart house is designed with a PV system, EV, HP, and solar collector (SC). Smart houses on the demand-side are incorporated with the thermal units and BESSs in the supply-side. The TS algorithm is applied as an optimization method to determine the optimal operation of thermal units and BESSs in the supply-side, and EVs and HPs of smart houses in the demand side. The BESSs satisfy the transmission constraints, and as well, the BESSs capacities are optimized by integrating with the controllable loads (EVs and HPs) of the smart houses. The proposed system is verified for different weather conditions (e.g. fair, cloudy and rainy days), along with different rates of demand-response such as 0%, 30%, and 50%. Furthermore, benefits for fifteen years operation of the proposed system in different weather and demand response conditions are evaluated. In addition, optimized capacities of batteries and inverters are determined. The effectiveness of the proposed system is verified by the numerical simulation using MATLAB® environment.

The outline of this paper is as follows: Section 2 depicts a brief

overview of the proposed smart grid model; Section 3 describes program formulation for the smart grid; Section 4 explains the optimal operation of the proposed smart grid system. Section 5 describes the simulation results and a conclusion is given in Section 6.

2. Smart grid configuration

Single line diagram of the proposed smart grid system is shown in Fig. 1. The power generation or supply-side of the smart grid consists of WGs (e.g. WG1, WG2, and WG3), PVs (e.g. PV1, PV2, and PV3), and thermal generators (e.g. GA, GB, GC, and GD) and BESSs (e.g. B1, B2, B3, and B4). Parameters of each thermal generator unit are shown in Table 1. The demand-side of the smart grid consists of residential houses and smart houses. From Fig. 1, there are seven different nodes (N1–N7) and each adjacent node is connected together with a transmission line. These nodes are considered as high voltage nodes (i.e. 7·2 kV). In node-1, WG1, PV1, and B1 are connected through step-up transformers and transmission lines. Thermal generators GA, GB, and GC are connected to the node-2, node-3 and node-4 through step-up transformers and transmission lines. Nodes-5 and 7 connect with similar types of power sources as node-1. In node-6, thermal generator, GD, and BESS, B3 are connected to the step-up transformers and transmission lines. All houses in each node are connected to the distribution buses (D1-D7). Distribution buses are considered as low voltage buses (i.e. 100 V). Therefore, each node is connected to a distribution bus by using a step-down transformer and a transmission line. Also, from Fig. 1, total load demand at time t is expressed as $PL(t)$. The fraction of load demand for each node is shown in Table 2. A smart house model is illustrated in Fig. 2 which includes EV, HP, PV, and SC. Parameters of the smart houses are shown in Table 3.

3. Program formulation for smart grid

In this section, the program formulation of the proposed smart grid is described. The different objective functions and constraints of the power supply-side and demand-side are presented in the following subsections.

3.1. Power supply-side formulation

The problem in this paper is represented by an optimization problem which is formulated by the following objective function and constraints.

(A) Objective function:

The supply-side of this paper considers BESSs and uses demand response to satisfy the transmission constraints. Therefore, the aim

Table 1
Parameters of each thermal units.

	Unit 1 ~ 6	Unit 7 ~ 9	Unit 10 ~ 12
P_{gi}^{max} [MW]	162	130	85
P_{gi}^{min} [MW]	25	20	25
a_i [$]	450	700	450
b_i [$/MW]	19.70	16.60	27.74
c_i [$/MW]	0.00398	0.002	0.00079
T_i^{on} [hour]	6	5	3
T_i^{off} [hour]	6	5	3
$cost_i$ [$]	1800	1100	520

Table 2
Load demand.

Node no.	1	2	3	4	5	6	7
Node Load P_{Li}	$\frac{P_L}{16}$	$\frac{P_L}{8}$	$\frac{P_L}{8}$	$\frac{P_L}{8}$	$\frac{P_L}{16}$	$\frac{P_L}{4}$	$\frac{P_L}{4}$

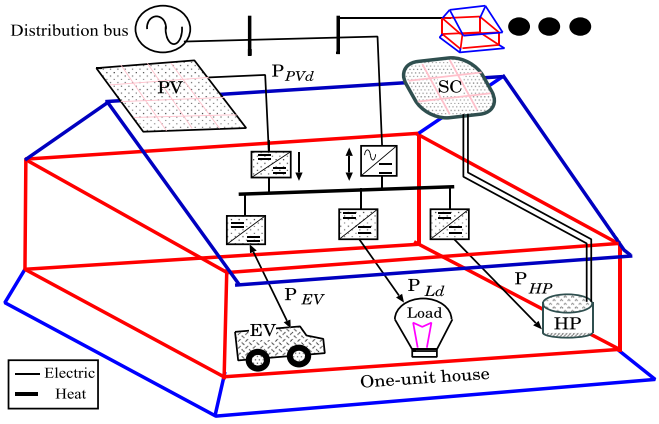

Fig. 2. Smart-house model.

Table 3
Smart house parameters.

Maximum power (P_{Ld})	3 kW
Inverter of EV (P_{EV})	3 kW
Capacity of EV (S_{EV})	15 kWh
Heat pump (P_{HP})	1.5 kW/4.5 kW
Photovoltaic (P_{PVd})	2 kW
Used hours of shower	19 ~ 22 h
Amount of Shower	100 L
Area of SC	1.6 m^2
Number of SC	3
Tank capacity	370 L

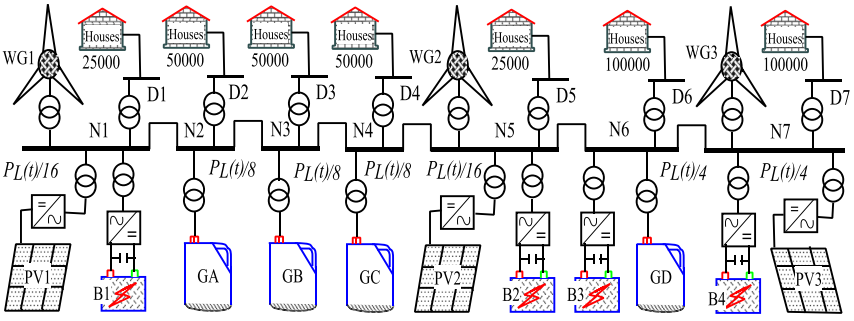

Fig. 1. Single line diagram of proposed smart grid system.

of the objective function is to maximize the benefits (max R) of the power supply-side.

$$\max R = TG_b - BESS_c \tag{1}$$

where TG_b and $BESS_c$ are the profits from the thermal generator during 15 years [$] and the BESS cost [$] respectively. The TG_b is represented as follows:

$$TG_b = (TG_{cw} - TG_{cd}) \times 365 \times 15 \tag{2}$$

where, TG_{cw} and TG_{cd} are the cost of thermal generator without demand response and with demand response respectively.

The $BESS_c$ is defined as follows:

$$BESS_c = \sum_{i=1}^{NB}(S_{Bi} \cdot CB) + \sum_{i=1}^{NI}(P_{Ii} \cdot CI) \tag{3}$$

where, S_{Bi}, P_{Ii}, CB, CI, NB, and NI are battery capacity [MWh], inverter capacity [MW], battery capacity cost [$/MWh], inverter capacity cost [$/MW], number of batteries and number of inverters, respectively.

The total cost of thermal generator units TG_c is determined from the following equation:

$$TG_c = \sum_{t=1}^{NT}\left\{\sum_{i=1}^{NG}\left(FC_i(P_{gi}(t)) + SUC_i(t)\right)\right\} \tag{4}$$

where NT, NG, $FC_i(P_{gi}(t))$, $P_{gi}(t)$, and SUC_i are total scheduling period [hours], total thermal generator units, fuel cost function [$] of unit i at hour t, output power of unit i at hour t and startup cost [$] of unit i at hour t, respectively. Fuel cost is formulated as a following quadratic function of the output power of thermal units that provides an accurate result of fuel cost [36,37]:

$$FC_i(P_{gi}(t)) = a_i + b_i P_{gi}(t) + c_i P_{gi}^2(t) \tag{5}$$

where, a_i, b_i, and c_i are fuel constants.

(B) Constraints:

Several constraints are considered for the power supply side i.e. the power balance constraint, thermal units constraints, and battery constraint.

(i) Power balance constraint

The summation of thermal units of output power, battery output power, PV output power, and wind generator output in each scheduling time t should correspond to the summation of load demand in each node P_{Li}.

$$\begin{aligned} P_L(t) &= \sum_{i=1}^{7} P_{Li}(t) \\ &= \sum_{i=1}^{12} P_{gi}(t) + \sum_{i=1}^{3} P_{WGi}(t) + \sum_{i=1}^{3} P_{PVi}(t) + \sum_{i=1}^{7} P_{PVdi}(t) \\ &\quad + \sum_{i=1}^{4} P_{Bi}(t) + \sum_{i=1}^{7} P_{EVi}(t) - \sum_{i=1}^{7} P_{HPi}(t) \end{aligned} \tag{6}$$

where P_{Li}, P_{gi}, P_{WGi}, P_{PVi}, P_{PVdi}, P_{Bi}, P_{EVi}, and P_{HPi} are the load demand [MW], thermal generator power [MW], WG power [MW], PV power in the supply side [MW], PV power in the demand side [MW], battery power [MW], EV battery power [MW], and HP power [MW], respectively.

(ii) Power limit constraint of thermal generator

The thermal generator power of unit i at hour t is constrained within the limits P_{gi}^{max} and P_{gi}^{min}.

$$P_{gi}^{min} \le P_{gi}(t) \le P_{gi}^{max} \tag{7}$$

where P_{gi}^{max} and P_{gi}^{min} are the thermal generator maximum power of unit i [MW] and the thermal generator minimum power of unit i [MW].

(iii) Minimum up or down time of units

Due to the operational limitations, once one unit is committed or uncommitted it should be kept stable for a minimum period of time before a transition. This leads to the following equations:

$$T_i^{on} \le X_i^{on}(t) \tag{8}$$

$$T_i^{off} \le X_i^{off}(t) \tag{9}$$

where T_i^{on}, T_i^{off}, X_i^{on} and X_i^{off} are the minimum up or down time [hour] and duration of being continuously ON or OFF [hour] of generating unit i.

(iv) Battery's power limit constraint

The power of each battery is constrained within the limits P_{Bi}^{max} and P_{Bi}^{min}.

$$P_{Bi}^{min} < P_{Bi} < P_{Bi}^{max} \tag{10}$$

where P_{Bi}^{max} and P_{Bi}^{min} are the battery's maximum power [MW] and minimum power [MW], respectively.

(v) State of charge limit constraint

The battery has a margin band of the state of charge, with an upper limit of 80% and lower limit of 20%. The reason behind that this is the over discharging and overcharging decrease the battery life [38]. Also, topping off a battery at a high state of charge is inefficient because of its internal resistance. Thus cycled battery applications tend to operate within a state of charge range of 20%–80% [39]. Therefore, the state of charge of each battery must be limited within a specified range.

$$S_{Bi}^{min}(=20[\%]) < S_{Bi} < S_{Bi}^{max}(=80[\%]) \tag{11}$$

where S_{Bi}, S_{Bi}^{max}, and S_{Bi}^{min} are the state of charge of battery [%], the maximum state of charge [%] and the minimum state of charge [%], respectively.

3.2. Program formulation in demand side

The EV and HP in the smart houses are considered the controllable loads of the smart grid. The objective function and the constraints for the optimization problem of the smart house are as follows:

(A) Objective function:

The objective function in this optimization problem is designed to minimize the transmission constraint violation.

$$\min F = \sum_{t\in T}\left(P_{fij}^{max} - \left|P_{fij}(t)\right|\right) \quad \left(\left|P_{fij}(t)\right| > P_{fij}^{max}\right) \tag{12}$$

where, P_{fij} and P_{fij}^{max} are the power flow between nodes i and j [MW] and the transmission constraints [MW], respectively. t is scheduling time and T is the total time.

(B) Constraints:

The constraints of the demand side i.e. EV battery constraints and HP constraints are considered.

(i) Power limit constraint of EV battery

The power of each EV battery is constrained within the limits of P_{EVi}^{max} and P_{EVi}^{min}.

$$P_{EVi}^{min} < P_{EVi} < P_{EVi}^{max} \tag{13}$$

where P_{EVi}^{max} and P_{EVi}^{min} are the EV battery maximum power [MW] and the EV battery minimum power [MW].

(ii) State of charge limit of EV battery

Similar to the battery, the state of charge limit of the EV battery is as follows:

$$S_{EVi}^{min}(=20[\%]) < S_{EVi} < S_{EVi}^{max}(=80[\%]) \tag{14}$$

where S_{EVi}, S_{EVi}^{max} and S_{EVi}^{min} are the state of charge of EV battery, maximum state of charge of EV battery [%], and minimum state of charge of EV battery [%], respectively.

(iii) Heat pump constraint

Each HP's output must be limited within a specified range.

$$P_{HPi} \le P_{HPi}^{max} \tag{15}$$

P_{HPi} and P_{HPi}^{max} are the HP power [MW] and the HP maximum power [MW] respectively. Each HP's storage water tank temperature must be 60° C by 19 O'clock.

$$T_{i(t=19)} > 60[^{\circ}\mathrm{C}] \tag{16}$$

$T_{i(t=19)}$ is the water temperature of storage tank at 19 O'clock for the HP in node i.

4. Optimal operation

The optimal operation of the smart grid in this paper is determined by the Tabu search. Optimal operations in the power supply side and power demand side are described in the following subsections 4.1 and 4.2, respectively.

4.1. Optimal operation in power supply side

A flow-chart of the power supply side is shown in Fig. 3. It is a thermal unit commitment program which considers the demand response. Different steps of this figure are described as follows:

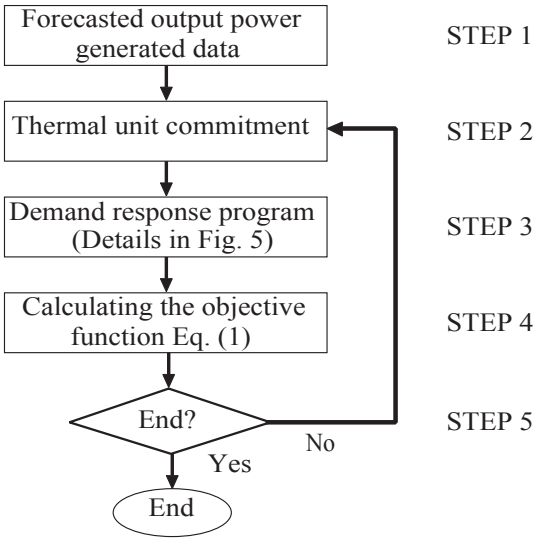

Fig. 3. Thermal unit commitment program with demand response.

Step 1 The forecast powers of WG P_{WG}, PV power on the supply side P_{PV}, PV power on the demand side P_{PVd}, and load demand P_L are determined.

Step 2 In order to satisfy the several constraints such as the minimum up or down time constraints, the thermal units output power constraint, EV constraint and battery constraint of the power supply side are produced. Fig. 4 shows the search approach of neighborhood solutions of the thermal unit generators. From this figure, the neighborhood solutions around the initial solution are searched in the time scheduling direction of thermal units. All thermal units in this paper are operated at rated power at all times. The thermal unit output power can be reduced by smart house operation.

Step 3 The controllable loads such as HP power and EV power are determined in order to minimize the quantity of violations of the transmission constraints (detailed in Section 4.2).

Step 4 The Tabu search algorithm is applied here. The neighborhood of thermal units solutions is evaluated, and the neighborhood solution which minimizes the thermal units total cost is recorded in the Tabu list.

Step 5 The terminating condition is verified. The termination condition is referred by the total number of iterations for Tabu Search. This paper is considered 300 iterations in order

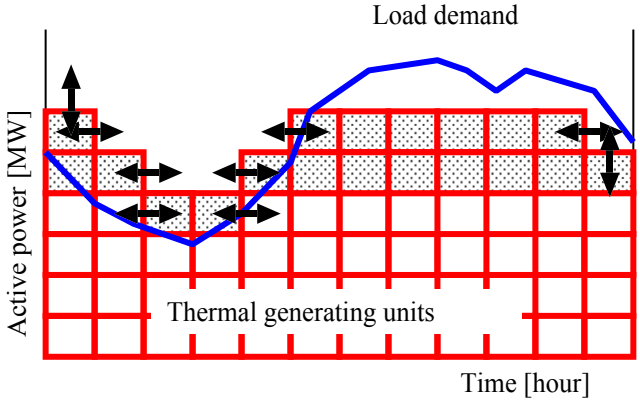

Fig. 4. Thermal unit commitment with demand response (STEP 2 in Fig. 3).

to achieve an optimal result. If the terminating condition is satisfied, the searching will be terminated. If it is not satisfied, the searching goes back to the STEP 2, and the search is progressed for the next iteration.

4.2. Optimal operation in the demand side

Fig. 5 shows the flow-chart for the optimal operation in the demand side, and the detailed algorithm is shown in this subsection. The solutions are determined for the HP and EV power. The neighborhood solution is the power of the HP for each scheduled time.

Step 1 The neighborhood solutions of thermal unit power P_g are determined.
Step 2 The scheduled time that the HP should be operated using the solar radiation forecast is created. The initial HP power $P_{H\,Pi}$ which satisfies the HP and EV constraints are produced.
Step 3 The Tabu search algorithm is applied here. The HPs neighborhood solutions P_{NEXTi} are determined near the initial HP solution $P_{H\,Pi}$.
Step 4 The power imbalance $(P_L(t) + \sum_{i=1}^{NH} P_{H\,Pi}(t) - \sum_{i=1}^{NG} P_{gi}(t))$ is determined for each neighborhood solution of HP's power P_{NEXTi} which is produced in STEP 3. It is shown in Fig. 6.
Step 5 The power flows in each node P_{fij} are calculated for each neighborhood solution of HP P_{NEXTi} which is produced in STEP 3. The power flows are calculated using the Algebraic method based on the load demand in each node, output power of thermal units, and output power of the HP.
Step 6 The violated quantity of transmission constraints and the power imbalance are minimized using the EV battery and the battery of the power supply side.

Power flow in violation of transmission constraints is minimized by the EV battery and the battery of the power supply side. If the power imbalance $(P_L(t) + \sum_{i=1}^{NH} P_{H\,Pi}(t) - \sum_{i=1}^{NG} P_{gi}(t))$ is negative (surplus power), the EV battery and battery are charged to compensate the power imbalance. If the EV battery and storage

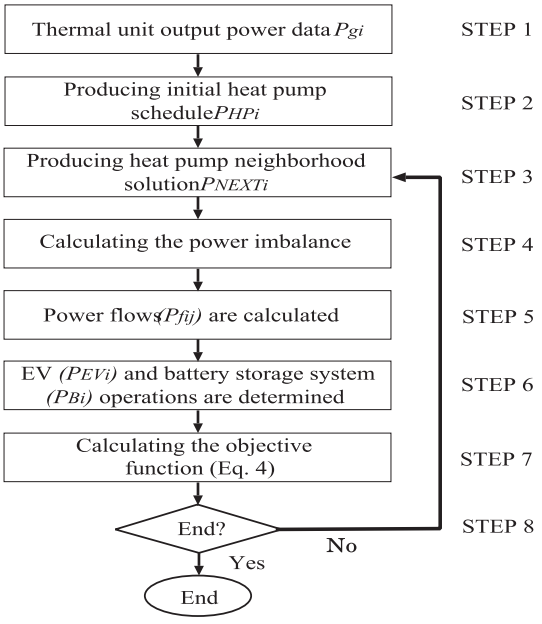

Fig. 5. Demand response program with transmission constraint.

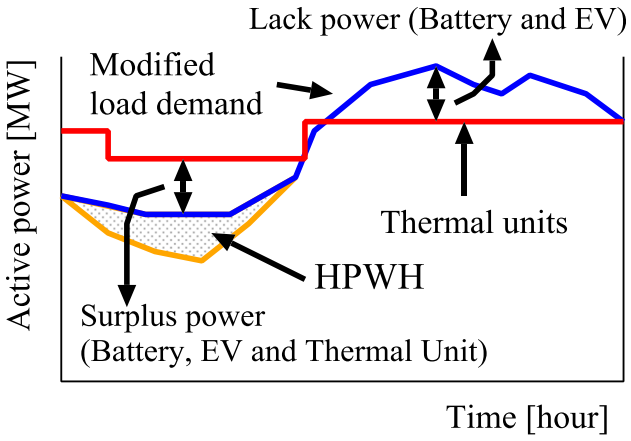

Fig. 6. Calculating the power imbalance (STEP 4 Fig. 5).

battery cannot compensate the power imbalance, thermal units output is decreased, and economic load dispatch is applied to the determination of thermal units output power. If the power imbalance is positive (lacking power), the EV battery and storage battery are discharged to compensate the power imbalance.

Step 7 The best neighborhood solution which minimizes the violated quantity of transmission constraints is recorded to the Tabu list.
Step 8 The terminating condition is verified. Similar to Fig. 3, this papers has considered the 300 iterations. If the terminating condition is satisfied, the searching will be terminated. If it is not satisfied, the searching goes back to the STEP 3, and the search is progressed for the next iteration.

5. Simulation results

Simulation Results are shown in this Section. The simulation has been performed by the MATLAB/Simulink. This paper has been considered the actual data from Miyakojima, Okinawa, Japan. Subsection 5.1 describes the simulation conditions or inputs of the proposed system. Subsections 5.2 and 5.3 show the optimal operation integrated with demand response and determined benefits of the proposed method with different demand responses, respectively. These subsections have reflected the outcomes of the proposed system.

5.1. Simulation conditions

The WGs output power, PVs output power in supply side and PVs output power in demand side are considered for the smart grid. Fig. 7(a)–(c) show the forecast of load demand, active power of PVs and WGs in the supply side, respectively. The active power of PVs in the supply has been considered by the average output power in a fair day. Fig. 7(d)–(f) show the PV output power in demand side for each weather condition. The battery and inverter costs are illustrated in Table 4 [40]. Table 5 illustrates the minimum capacities of battery and inverter i.e. 12 MWh and 2 MW respectively. Battery and inverter capacities are changed by multiplying variables with the minimum capacities of battery and inverter. Also, these capacities can be optimized by using the minimum capacities of battery and inverter. The demand side of the proposed smart grid is constructed with a large number of residential and smart houses. The demand-response operation is integrated with the thermal units commitment to satisfy the transmission constraints. The optimum capacities of the battery and inverter are verified in the

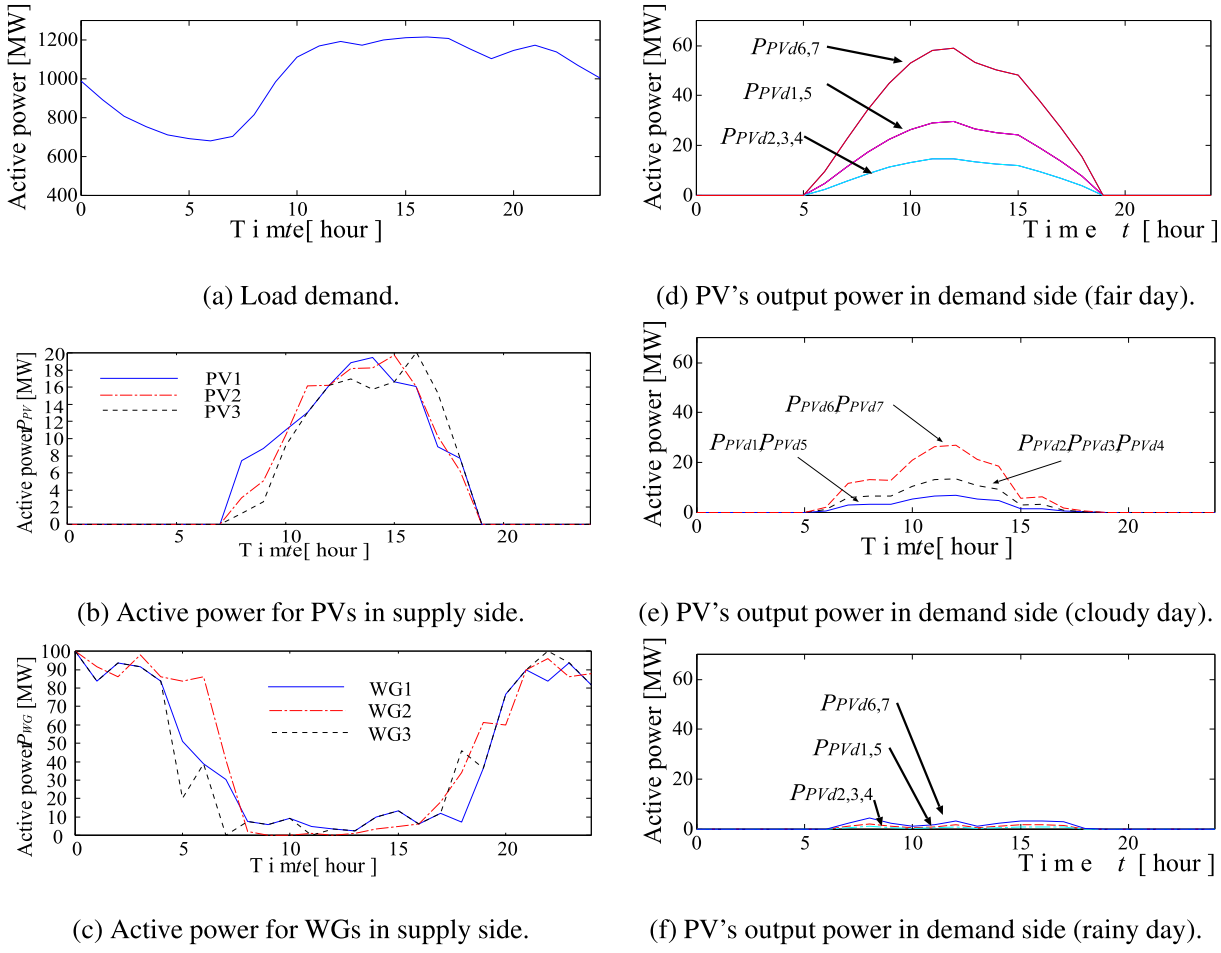

(a) Load demand.

(d) PV's output power in demand side (fair day).

(b) Active power for PVs in supply side.

(e) PV's output power in demand side (cloudy day).

(c) Active power for WGs in supply side.

(f) PV's output power in demand side (rainy day).

Fig. 7. Simulation condition.

Table 4
NaS battery and inverter cost.

NaS battery capacity cost *CB*	312.5 $/kWh
Inverter capacity cost *CI*	837.5 $/kW

Table 5
Capacity of battery and inverter.

	Battery1	Battery2	Battery3	Battery4
P_I^{max}[MW]	2 × variables (1, 2, 3 ⋯)			
S_B^{max}[MWh]	12 × variables (1, 2, 3 ⋯)			

cases of 0%, 30%, and 50% rates of demand response. The number of residential houses, smart houses, and rates of demand response are shown in Table 6. In the smart grid system, residential houses consist of similar components as a smart house expect the EV. In this Table, the 0% rate of demand response means that the transmission constraint is satisfied only by the BESS in the power supply side. Three different types of weather conditions such as fair, cloudy, and rainy days are considered for the power system simulation. The conventional method does not consider demand response or the BESS in the power supply side. Transmission constraints are shown in Table 7. This subsection reflects simulation conditions and inputs of the proposed system.

Table 6
Demand-side of the proposed system.

Node	Total house number	Demand response system rate			
		Smart house number	0%	30%	50%
1	25,000	12,500	0	7500	12,500
2	50,000	25,000	0	15,000	25,000
3	50,000	25,000	0	15,000	25,000
4	50,000	25,000	0	15,000	25,000
5	25,000	12,500	0	7500	12,500
6	100,000	50,000	0	30,000	50,000
7	100,000	50,000	0	30,000	50,000

Table 7
Transmission constraint.

	Transmission constraints [MW]
Node 12 (P_{f12})	70
Node 56 (P_{f56})	330

5.2. Optimal operation integrated with demand response system

Fig. 8 illustrates the optimal operation of the thermal unit integrated with 50% demand response on a cloudy day. Fig. 8(a) shows the required power of the HPs. From this figure, HPs are almost operated in the night-time because that time load is lower than the daytime. Fig. 8(b) shows the water temperature of the

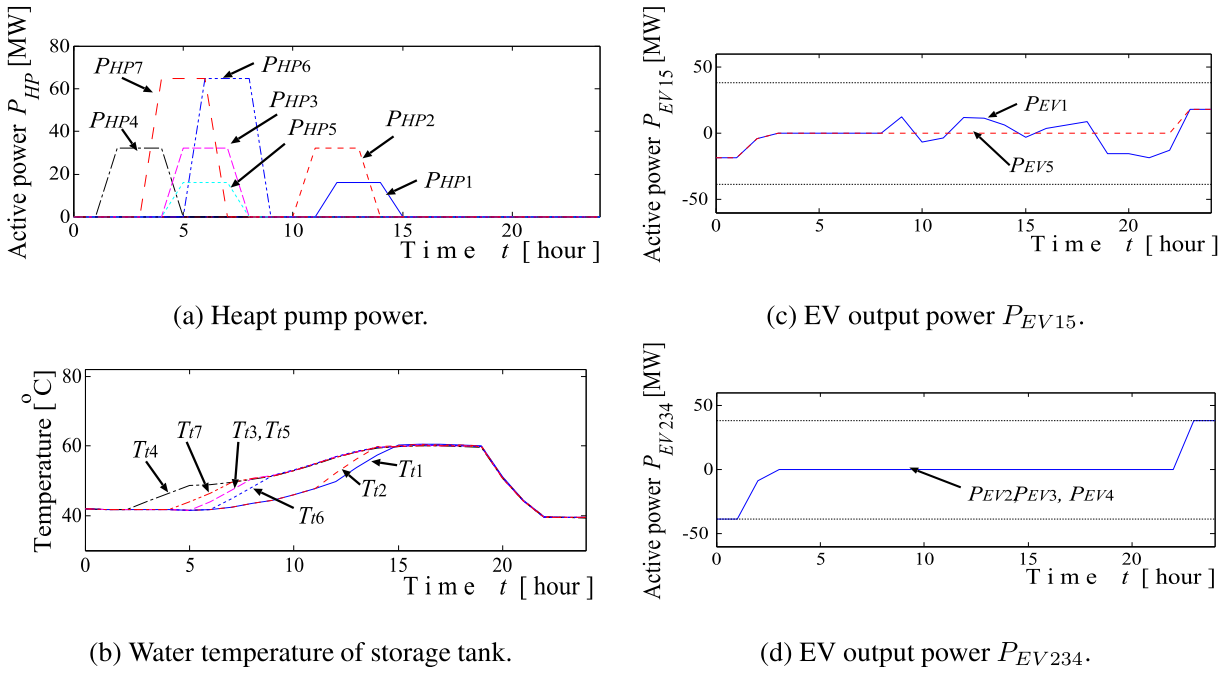

(a) Heapt pump power.

(b) Water temperature of storage tank.

(c) EV output power P_{EV15}.

(d) EV output power P_{EV234}.

Fig. 8. Simulation results in cloudy day in 50% demand response system rate.

storage tank. The water in the storage tank is heated up to 60° C at 19 Oclock by using the HP. Therefore, it satisfies the HP constraints.) (Fig. 8(c)–(e) and Fig. 8(f) show the output power of the EV batteries and the state of charge of EV batteries, respectively. Charge/discharge of EV batteries can reduce the operation of the thermal units and satisfy the transmission constraints. The charging and discharging of EV batteries are indicated by the negative and positive values in) (Fig. 8(c)–(e). The state of charge of EV batteries is kept within the specific range in Fig. 8(f). The output power and state of charge of the BESS are shown in Fig. 8(g) and (h), respectively. The BESSs also satisfy the state of charge constraints. Fig. 8(i) shows the output power of thermal units for the conventional method which reflects that only thermal units supply electricity to the load demand. Fig. 8(j) shows the output power of thermal units for the proposed method which is integrated with the demand response to supply electricity to the load demand. In Fig. 8(i) and (j), P_{LH} is load demand with required power of HP, P_{Lm} is load demand without required power of HP, P_g is the generation power of thermal units. From these figures, the peak load in daytime is reduced, and the thermal units which have low efficiency are uncommitted by introducing the demand response in the proposed system. Therefore, the reduction of the thermal units operation leads to lessening of the total cost of the power system. Fig. 8(k) and (l) illustrate the power flow in node 1–2 and node 5–6. From these figures, the transmission constraints are violated only the operations of thermal units (non-demand response). The demand response system can optimize the violated power flows within the specified range, and the transmission constraints are satisfied.

5.3. Determined benefits of the proposed method with different demand responses

The benefit R of 15 years duration in different rates of demand response are illustrated in Table 8. The calculation process of benefit R has been described in Equation (1)–(3). Different rates of demand response (e.g. 0%, 30%, and 50%) and weather conditions (e.g. fair, cloudy, and rainy) are considered for the calculation of benefit R. From this Table, the benefits R for cloudy and rainy days are lower as compared with the fair day. Due to the lack of solar insulation in cloudy and rainy days, the HPs are required to operate for heating the storage water. Operations of the HPs increase the power flow in node 1–2 and node 5–6. Therefore, the EV battery and storage battery are scheduled to satisfy the transmission constraints. As a result, the benefit R decreases in cloudy and rainy days. On the other hand, when rates of demand response are increased, the benefit R is increased too, because high rates of demand response can reduce the battery and inverter capacities. Table 9 illustrates the optimum capacities of battery and inverter which can maximize the benefit R in different rates of demand-response and weather conditions. From this Table, the optimum capacities of the battery and inverter are decreased on the fair day with a 50% demand response rate. In fair days, sufficient solar insulation is available, therefore, the SC can heat the storage water. Hence, it can reduce the HP operation consequently, battery and inverter capacities are reduced on a fair day.

The benefit R for different rates of demand response are shown in Fig. 9. In this case, the weather condition is considered from 15 years of historical data of Miyakojima, Okinawa, Japan. From this figure, the benefit R is increased within the large rates of demand response for reducing capacities of the battery and inverter. The total benefit R and optimum capacity of battery and inverter are shown in Table 10 within different rates of demand response. Different capacities of battery and inverter were shown in Table 5, which has been optimized from the demand response program (Fig. 5). From Table 10, the benefit R in 15 years is negative for a rate of 0% demand response. The reason behind this is that only the BESSs in the supply-side satisfies the transmission constraints, therefore, battery and inverter capacities are increased. As a result, the power generation costs increase. From this Table, it is also shown that the benefit R is increased when the rate of demand response is raised because it reduces the capacities of the battery and inverter.

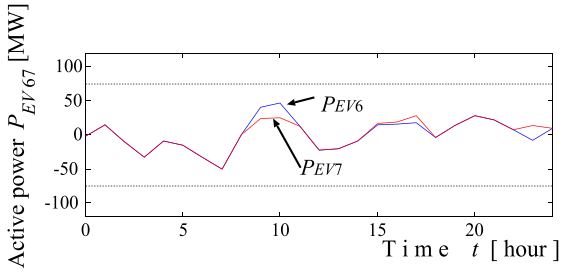

(e) EV output power P_{EV67}.

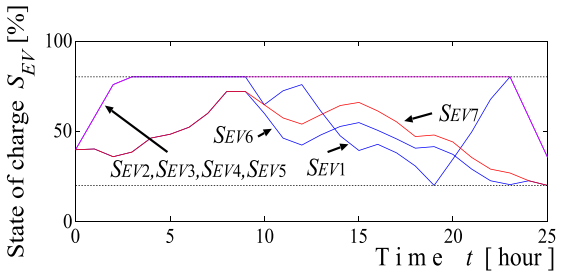

(f) State of charge of EV S_{EV}.

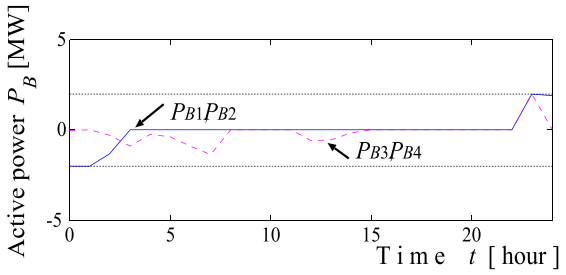

(g) Battery output power P_B.

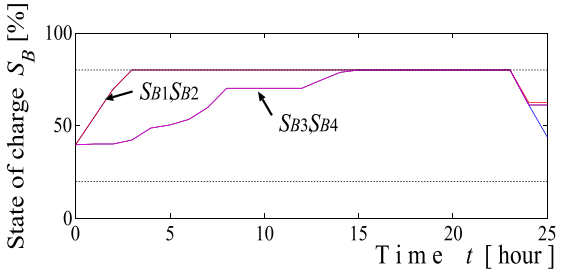

(h) State of charge of battery S_B.

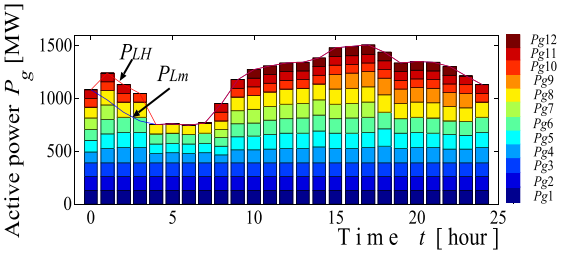

(i) Output power of thermal units in conventional P_g.

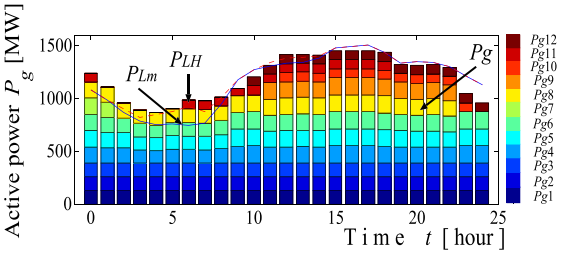

(j) Output power of thermal units in demand response system P_g.

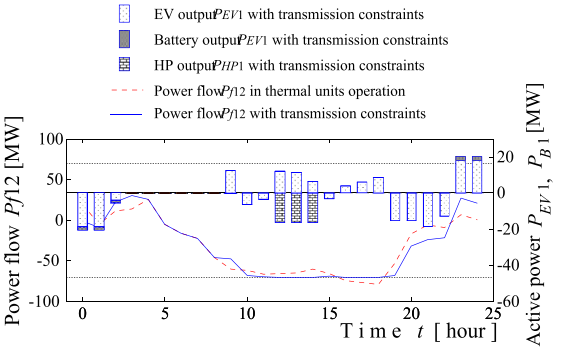

(k) Power flow P_{f12}.

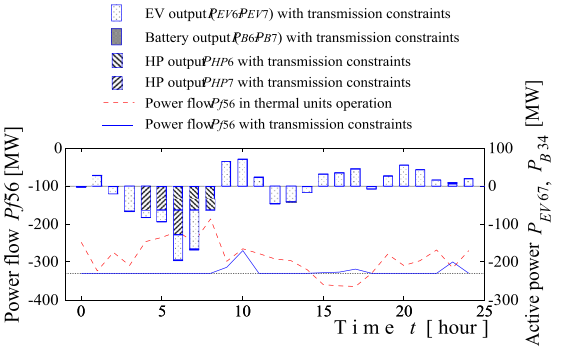

(l) Power flow P_{f56}.

Fig. 8. (*continued*).

Table 8
Benefit R in 15 years.

Benefit rate R [$] in 15 years			
Demand response system rate	Weather conditions		
	Fair	Cloudy	Rainy
0% (Battery only)	5,760,000	−98,000,000	−366,350,000
30%	52,450,000	22,900,000	31,840,000
50%	52,450,000	49,640,000	41,410,000

Table 9
Optimum capacity of inverter and battery.

Demand response system rate	Weather conditions					
	Fair	Cloudy	Rainy	Fair	Cloudy	Rainy
	Inverter capacity			Battery capacity		
	P_I^{max} [MW]			S_B^{max}[MWh]		
0% (Battery only)	16	72	136	48	384	864
30%	8	8	16	48	48	48
50%	8	8	24	48	48	48

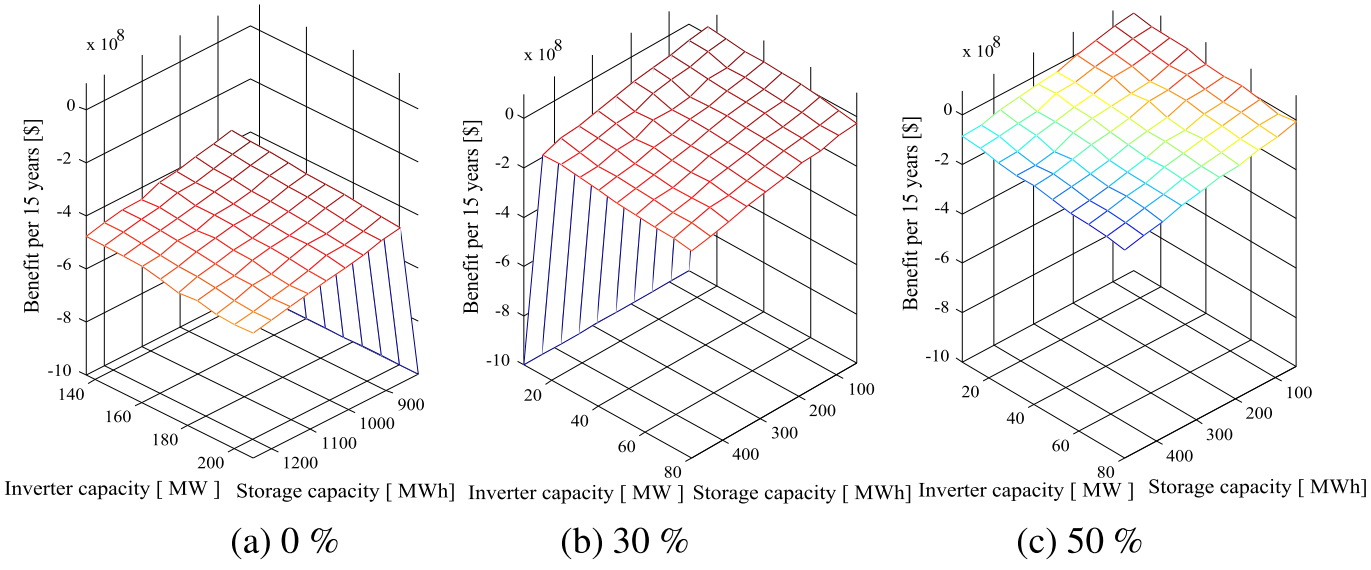

Fig. 9. Benefit in 15 years in each participation rate of demand response.

Table 10
Benefit R of 15 years with optimum capacity of inverter and battery.

Demand response system rate	Benefit R [$] in 15 years	Inverter capacity P_I^{max} [MW]	Battery capacity S_B^{max}[MWh]
0% (Battery only)	−312,990,000	136	864
30%	32,650,000	16	48
50%	46,060,000	8	48

6. Conclusion

A distributed generators based smart grid system has been proposed. The transmission constraints are satisfied by the demand response which can optimize the BESS and inverter. The demand response system also reduces the operation of inconvenient thermal units. The controllable loads (i.e. EV and HP) of the smart houses in the demand side are utilized to satisfy the transmission constraints. As a results, the proposed system can reduce the capacities of the battery and inverter. Simulation results are considered in different weather conditions and demand response rate. The optimum capacities of the battery and inverter are determined for different cases. From the simulation results, the proposed method can satisfy the transmission constraints of the smart grid. The benefit for 15 years operation of the smart grid is calculated for the proposed method. The benefits of smart grid are increased significantly when demand response is considered.

References

[1] A. Al-Sabounchi, J. Gow, M. Al-Akaidi, Simple procedure for optimal sizing and location of a single photovoltaic generator on radial distribution feeder, IET Renew. Power Gener. 8 (2) (2014) 160–170.
[2] M. Silva, H. Morais, Z. Vale, An integrated approach for distributed energy resource short-term scheduling in smart grids considering realistic power system simulation, Energy Convers. Manag. 64 (2012) 274–288.
[3] E.C. Christina, B. Paul, M.H. Robert, R.S. David, Implications of widespread algal biofuels production on macronutrient fertilizer supplies: nutrient demand and evaluation of potential alternate nutrient sources, Appl. Energy 143 (2015) 7180.
[4] A.M. Rachel, R.B. John, Energy price risk and the sustainability of demand side supply chains, Appl. Energy 123 (2014) 327334.
[5] A. Ghafouri, J. Milimonfared, G.B. Gharehpetian, Coordinated control of distributed energy resources and conventional power plants for frequency control of power systems, IEEE Trans. Smart Grid 6 (1) (2014) 104–114.
[6] B. Sahand, P.C. David, C. Curran, D. Ned, Renewable resources portfolio optimization in the presence of demand response, Appl. Energy 162 (2016) 139–148.
[7] D.K. Christos, B. Simone, M. Iakovos, B.K. Elias, Occupancy-based demand response and thermal comfort optimization in microgrids with renewable energy sources and energy storage, Appl. Energy 163 (2016) 93104.
[8] J. Bekkering, E.J. Hengevelda, W.J.T. Gemert, A.A. Broekhuisa, Designing a green gas supply to meet regional seasonal demand – an operations research case study, Appl. Energy 143 (2015) 348358.
[9] L. Wu, D. Infield, Power system frequency management challenges a new approach to assessing the potential of wind capacity to aid system frequency stability, IET Renew. Power Gener. 8 (7) (2014) 733–739.
[10] P. Dieter, R. Glenn, B. Kenneth, P. Christina, D. Erik, D. William, S. Dirk, H. Lieve, CO_2-abatement cost of residential heat pumps with active demand response: demand- and supply-side effects, Appl. Energy 156 (2015) 490501.
[11] S. Javier, M.K. Georgios, N.P. Efstratios, E. Antonio, A rolling horizon optimization framework for the simultaneous energy supply and demand planning in microgrids, Appl. Energy 155 (2015) 485501.
[12] Y. Wu, V.K.N. Lau, D.H.K. Tsang, L.P. Qian, L. Meng, Optimal energy scheduling for residential smart grid with centralized renewable energy source, IEEE Syst. J. 8 (2) (2013) 562–576.
[13] I. Lampropoulos, N. Baghina, W.L. Kling, P.F. Ribeiro, A predictive control scheme for real-time demand response applications, IEEE Trans. Smart Grid 4 (4) (2013) 2049–2060.
[14] Y. Xu, W. Zhang, G. Hug, S. Kar, Z. Li, Cooperative control of distributed energy storage systems in a microgrid, IEEE Trans. Smart Grid 6 (1) (2014) 238–248.
[15] S. Sreejith, S.P. Simon, M.P. Selvan, Analysis of FACTS devices on security constrained unit commitment problem, Int. J. Electr. Power & Energy Syst. 66 (2015) 280–293.
[16] F. Genoese, M. Genoese, M. Wietschel, Medium-term flexibility options in a power plant portfolio-Energy storage units vs. thermal units, in: 9th International Conference on the European Energy Market (EEM), 2012, pp. 1–9.
[17] H. Dawei, T. Zhenyu, R.G. Harley, Chance constrained unit commitment with wind generation and superconducting magnetic energy storages, in: 2012 IEEE Power and Energy Society General Meeting, 2012, pp. 1–6. San Diego, CA.
[18] F. Diaz-Gonzalez, A. Sumper, O. Gomis-Bellmunt, R. Villafafila-Robles, A review of energy storage technologies for wind power applications, Renew. Sustain. Energy Rev. 16 (2012) 215471.
[19] M. Kintner-Meyer, M. Elizondo, P. Balducci, V. Viswanathan, C. Jin, X. Guo, T. Nguyen, F. Tuffner, Energy Storage for Power Systems Applications: a Regional Assessment for the Northwest Power Pool (NWPP), US Department of Energy, 2010.
[20] S. Carr, G.C. Premier, A.J. Guwy, R.M. Dinsdale, J. Maddy, Energy storage for active network management on electricity distribution networks with wind

power, IET Renew. Power Gener. 8 (3) (2014) 249–259.
[21] J.H. Zheng, J.J. Chena, Q.H. Wu, Z.X. Jing, Reliability constrained unit commitment with combined hydro and thermal generation embedded using self-learning group search optimizer, Energy 81 (2015) 245254.
[22] S. Chakraborty, T. Ito, T. Senjyu, A.Y. Saber, Unit commitment strategy of thermal generators by using advanced fuzzy controlled binary particle swarm optimization algorithm, Int. J. Electr. Power & Energy Syst. 3 (1) (2012) 1072–1080.
[23] C. Shao, X. Wang, X. Wang, C. Du, C. Dang, S. Liu, Cooperative dispatch of wind generation and Electric vehicles with battery storage capacity constraints in SCUC, IEEE Trans. Smart Grid 5 (5) (2014) 2219–2226.
[24] C. Fernandes, P. Frias, J.M. Latorre, Impact of vehicle-to-grid on power system operation costs: the Spanish case study, Appl. Energy 96 (2012) 194–202.
[25] T. Ghanbarzadeh, S. Goleijani, M.P. Moghaddam, Reliability constrained unit commitment with electric vehicle to grid using hybrid particle swarm optimization and Ant colony optimization, in: 2011 IEEE Power and Energy Society General Meeting, 2011, pp. 1–7. San Diego, CA.
[26] A.E. Kherameh, M. Aien, M. Rashidinejad, M. Fotuhi-Firouzabad, A particle swarm optimization approach for robust unit commitment with significant vehicle to grid penetration, in: 2014 Iranian Conference on Intelligent Systems (ICIS), 2014, pp. 1–6.
[27] A.Y. Saber, G.K. Venayagamoorthy, Intelligent unit commitment with vehicle-to-grid-A cost-emission optimization, J. Power Sources 195 (3) (2010) 898–911.
[28] M. Rahmani-Andebili, A. Abdollahi, M.P. Moghaddam, An investigation of implementing emergency demand response program (EDRP) in unit commitment problem, in: 2011 IEEE Power and Energy Society General Meeting, 2011, pp. 1–7. San Diego, CA.
[29] A. Khodaei, M. Shahidehpour, S. Bahramirad, SCUC with hourly demand response considering intertemporal load characteristics, IEEE Trans. Smart Grid 2 (3) (2011) 564–571.
[30] H. Falsafi, A. Zakariazadeh, S. Jadid, The role of demand response in single and multi-objective wind-thermal generation scheduling: a stochastic programming, Energy 64 (1) (2014) 853–867.
[31] C. Zhao, J. Wang, J.P. Watson, Y. Guan, Multi-stage robust unit commitment considering wind and demand response uncertainties, IEEE Trans. Power Syst. 28 (3) (2013) 2708–2717.
[32] C.L. Chen, Key issues of wind capacity integration in congested areas of the Taiwan power system, IET Renew. Power Gener. 8 (1) (2014) 10–21.
[33] F. Rahimi, A. Ipakchi, Demand response as a market resource under the smart grid paradigm, IEEE Trans. Smart Grid 1 (1) (2010) 82–88.
[34] H.O.R. Howlader, H. Matayoshi, T. Senjyu, Thermal units commitment integrated with reactive power scheduling for the smart grid considering voltage constraints, Int. J. Emerg. Electr. Power Syst. 16 (4) (2015) 323–330.
[35] M. Gendreau, An Introduction to Tabu Search, Universite de Montreal, Canada, July 2002.
[36] D.P. Kothari, J.S. Dhillon, Power System Optimization, Prentice Hall of India, New Delhi, 2006.
[37] A. Zerigui, L.A. Dessaint, R. Hannat, R.T.F. Ah King, I. Kamwa, Statistical approach for transient stability constrained optimal power flow, IET Gener. Transm. Distrib. 9 (14) (2015) 1856–1864.
[38] A.M. Howlader, Y. Izumi, A. Uehara, N. Urasaki, T. Senjyu, A. Yona, A.Y. Saber, A minimal order observer based frequency control strategy for an integrated wind-battery-diesel power system, Energy 46 (2012) 16878.
[39] National Research Council, Personal Cars and China, Chinese academy of Engineering, The National Academic Press, Washington, D.C, 2003.
[40] NGK INSULATORS, LTD, http://www.ngk.co.jp/.